PHYSICAL REVIEW D **88,** 023532 (2013)

Thawing models in the presence of a generalized Chaplygin gas

Sergio del Campo,[1,*] Carlos R. Fadragas,[2,†] Ramón Herrera,[1,‡] Carlos Leiva,[3,§] Genly Leon,[1,‖] and Joel Saavedra[1,¶]

[1]*Instituto de Física, Pontificia Universidad de Católica de Valparaíso, Casilla 4950, Valparaíso, Chile*

[2]*Departamento de Física, Universidad Central de Las Villas, 54830 Santa Clara, Cuba*

[3]*Departamento de Física, Universidad de Tarapacá, Avenida General Velásquez 1775, Código Postal 1000007, Arica, Chile*

(Received 5 April 2013; published 26 July 2013)

In this paper we consider a cosmological model whose main components are a scalar field and a generalized Chaplygin gas. We obtain an exact solution for a flat arbitrary potential. This solution have the right dust limit when the Chaplygin parameter $A \to 0$. We use the dynamical systems approach in order to describe the cosmological evolution of the mixture for an exponential self-interacting scalar field potential. We study the scalar field with an arbitrary self-interacting potential using the ''Method of f-devisers.'' Our results are illustrated for the special case of a coshlike potential. We obtain that the usual scalar-field-dominated and scaling solutions cannot be late- time attractors in the presence of the Chaplygin gas (with $\alpha > 0$). We recover the standard results at the dust limit ($A \to 0$). In particular, for the exponential potential, the late-time attractor is a pure generalized Chaplygin solution mimicking an effective cosmological constant. In the case of arbitrary potentials, the late-time attractors are de Sitter solutions in the form of a cosmological constant, a pure generalized Chaplygin solution or a continuum of solutions, when the scalar field and the Chaplygin gas densities are of the same orders of magnitude. The different situations depend on the parameter choices.

DOI: 10.1103/PhysRevD.88.023532 PACS numbers: 98.80.Cq

I. INTRODUCTION

It is common knowledge that the expansion of the Universe is currently passing through an accelerated phase [1,2]. All the observational data from these former references until the current measurements of redshift and luminosity-distance relations of type Ia supernovae (SNe) [3] are in agreement with this accelerated era. These observations are indicating the presence of a vacuum energy, the well-known cosmological constant [4–6]. Another possible description is the existence of the scalar field that is evolving in a universe described by a Friedmann-Robertson-Walker (FRW) geometry, the quintessence model [7]. The current acceleration of the universe is one of the important problems of modern cosmology. This problem appears in Einstein's standard general relativity, and one of the proposals to solve it, within this framework, is to consider one exotic component in the matter content of the universe [8], the so-called dark energy component (for a review about this, see Ref. [9]). We would like to focus our attention on models where dark energy is described by a homogeneous scalar field ($\phi(t)$) [10]. In order to describe the dynamics of dark energy (quintessence), the equation of state parameter (EOS), $\omega_\phi \equiv p_\phi/\rho_\phi$ plays a crucial role. Its current value is close to -1. Therefore, the cosmic evolution of dark energy through the scalar field is described by the barotropic parameter ω_ϕ. In Ref. [11], the authors distinguished between two categories, the freezing ($d\omega_\phi/d\phi < 0$) and thawing ($d\omega_\phi/d\phi > 0$) models. These quintessence models are characterized by a scalar field potential that asymptotically goes to zero [12]. There are several references about this kind of cosmological model (for a summary, see Ref. [13]). On the other hand, Chaplygin gas models have been widely investigated in the literature [14–26]. The modified Chaplygin gas for the $k = 0$ FRW universe is exactly the same as adding a bulk viscosity proportional to a power of the fluid density [27,28]. The generalized Chaplygin gas (GCG) has been investigated from the dynamical systems viewpoint, for example, in [29–33].

In this paper we would like to extend the analysis in [12] by considering a more general matter component, namely, a GCG and a scalar field characterized by its self-interacting scalar potential. We obtain an exact solution for a flat arbitrary potential, which has the right dust limit when the Chaplygin parameter $A \to 0$ [12]. In order to motivate the analysis for a general (arbitrary) potential, we first consider the simple case of an exponential potential $V(\phi) = V_0 e^{-\lambda\phi}$ [34–54]. Then, we study an arbitrary self-interacting scalar field potential. In this case we use the ''Method of f-devisers'' presented in [55]. This method allows us to perform the phase space analysis without specifying the potentials *ad initium*, and then one just substitute the desired forms, instead of repeating the whole procedure for every distinct potential. The method is

*sdelcamp@ucv.cl
†fadragas@uclv.edu.cu
‡ramon.herrera@ucv.cl
§cleivas@uta.cl
‖genly.leon@ucv.cl
¶Joel.Saavedra@ucv.cl

a refinement of a method that has been applied to isotropic (FRW) scenarios [54,56–60], and that has been generalized to several cosmological contexts [61–64].

This article is organized as follows. In Sec. II we present the cosmological model under consideration. Section III is devoted to the study of the exponential potential an the corresponding dynamical system. In Sec. IV we study the phase space of the cosmological model for general potential $V(\phi)$. Finally, we conclude in Sec. V.

II. THE COSMOLOGICAL MODEL

In this section we would like to describe a cosmological setting composed of a minimally-coupled scalar field that describes the dark energy and a Chaplygin gas that behaves as dark matter in the appropriate limit.

The cosmological equations are given by

$$H^2 - \frac{\rho_{\rm ch} + \rho_\phi}{3} = 0, \tag{1}$$

$$\dot{\rho}_{\rm ch} + 3H(\rho_{\rm ch} + P_{\rm ch}) = 0, \tag{2}$$

$$\dot{\rho}_\phi + 3H(\rho_\phi + P_\phi) = 0, \tag{3}$$

where we work in units in which $8\pi G = 1$, H is the Hubble constant, and $\rho_{\rm ch}$ and ρ_ϕ are the Chaplygin gas and scalar field densities, respectively. For simplicity, the radiation component is neglected. $P_{\rm ch}$ and P_ϕ represent the Chaplygin gas and scalar field pressures, respectively. For the scalar field we have

$$\rho_\phi = \frac{\dot{\phi}^2}{2} + V(\phi), \tag{4}$$

$$P_\phi = \frac{\dot{\phi}^2}{2} - V(\phi). \tag{5}$$

On the other hand, the EOS for the GCG is

$$P_{\rm ch} = -\frac{A}{\rho_{\rm ch}^\alpha}, \tag{6}$$

where A is a positive constant and α is a constant with an upper bound, $\alpha \leq 1$, especially when $\alpha = 1$ corresponds to the original Chaplygin gas. In the framework of FRW cosmology, this EOS leads, after being inserted into the relativistic energy conservation equation, to an evolution of the energy density as

$$\rho_{\rm ch} = \left(A + \frac{B}{a^{3(\alpha+1)}}\right)^{\frac{1}{\alpha+1}} = \rho_{\rm ch0}\left[B_s + \frac{(1-B_s)}{a^{3(\alpha+1)}}\right]^{\frac{1}{\alpha+1}}. \tag{7}$$

Here, a is the scale factor and B is a positive integration constant. In this way, the GCG is characterized by two parameters, $B_s = A/\rho_{\rm ch0}^{1+\alpha}$ and α. Here, $\rho_{\rm ch0}$ is the current value of $\rho_{\rm ch}$, considering that $a = 1$ at the present. These parameter has been confronted with the observational data, see Refs. [65,66]. In particular, the values of $B_s = 0.73^{+0.06}_{-0.06}$ and $\alpha = -0.09^{+0.15}_{-0.12}$ were obtained in Ref. [66]. Also, in Ref. [14] the values $0.81 \lesssim B_s \lesssim 0.85$ and $0.2 \lesssim \alpha \lesssim 0.6$ were found from the observational data arising from different collaborations, namely, Archeops (by using the first peak localization) and BOOMERANG (by using the third peak localization). Recently, the values $B_s = 0.775^{+0.0161+0.037}_{-0.0161-0.0338}$ and $\alpha = 0.00126^{+0.000970+0.00268}_{-0.00126-0.00126}$ were obtained using the Markov chain Monte Carlo method [67]. For the phase space simulations implemented in the present paper, we select the value $\alpha = 0.5$, first in agreement with Archeops and BOOMERANG Collaborations, and second, following Ref. [68]. This value seems to be large in comparison with the observational values in [67]; however, if we consider large values for α, and include the effect of shear and rotation, then when studying the evolution of the perturbations in the GCG universes, it is found that the joint effect of shear and rotation is that of slowing down the collapse with respect to the simple spherical collapse model. The described effect allows to solve the instability problems of the so-called unified dark matter models at the linear perturbation level [68].

The evolution of the energy density $\rho_{\rm ch}$ shows the behaviors of GCG at different times. At early times, the energy density behaves as matter, while at late times it behaves like a cosmological constant. Then, this GCG in principle describes both dark matter and dark energy in a single matter component.

Now we can define the barotropic index $\omega_{\rm ch}$,

$$\omega_{\rm ch} = -\frac{A}{A + \frac{B}{a^{3(\alpha+1)}}}. \tag{8}$$

At late times, the universe is dominated by the scalar field and the GCG, neglecting the radiation component.

Equations (2) and (3) can be rewritten in terms of the auxiliary variables x, y and s, defined by

$$x = \frac{\phi'}{\sqrt{6}}, \qquad y = \sqrt{\frac{V(\phi)}{3H^2}}, \qquad s = -\frac{1}{V}\frac{dV}{d\phi}, \tag{9}$$

where the prime denotes derivatives with respect to $\tau = \ln a$. Considering that the contribution for the kinetic and potential energy are given by x^2 and y^2 respectively, the density parameter of the scalar field is given by

$$\Omega_\phi = \frac{\rho_\phi}{3H^2} = x^2 + y^2; \tag{10}$$

therefore, the equation of state is

$$\gamma = 1 + \omega = \frac{2x^2}{x^2 + y^2}. \tag{11}$$

Thus, inserting the auxiliary variables (9) into the equations of motions (1)–(3) we arrive to the following system

$$x' = -3x - \sqrt{\frac{3}{2}} s y^2 + \frac{3x}{2}\{2x^2 + (1 - x^2 - y^2)(1 + \omega_{\rm ch})\}, \tag{12}$$

$$y' = -\sqrt{\frac{3}{2}} s x y + \frac{3y}{2}\{2x^2 + (1 - x^2 - y^2)(1 + \omega_{\rm ch})\}, \tag{13}$$

$$s' = -\sqrt{6} s^2 (\Gamma - 1) x, \tag{14}$$

where

$$\Gamma \equiv V\left[\frac{dV}{d\phi}\right]^{-1} \frac{d^2V}{d\phi^2}. \tag{15}$$

Besides, the Friedmann constraint equation can be written as $\Omega_\phi + \Omega_{\rm ch} = 1$, and this implies $0 \leq \Omega_\phi \leq 1$, for a non-negative density. Therefore the dynamical evolution of (12)–(14) leave the coordinates (x, y) within the upper-half unit disc.

Furthermore, the system (12)–(14) is nonautonomous since

$$\omega_{\rm ch} = -\frac{A}{A + Be^{-3(\alpha+1)\tau}}, \tag{16}$$

and it is in general not closed since Γ does not depends *a priori* on the state variables x, y, s.

Before to perform a detailed analysis of the stability of this dynamical system we rewrite it in terms of the observable quantities Ω_ϕ and γ, and the new equations are given by

$$\gamma' = -3\gamma(2 - \gamma) + s(2 - \gamma)\sqrt{3\gamma\Omega_\phi}, \tag{17}$$

$$\Omega_\phi' = 3(1 - \gamma)\Omega_\phi(1 - \Omega_\phi) + 3\Omega_\phi(1 - \Omega_\phi)\omega_{\rm ch}, \tag{18}$$

$$s' = -\sqrt{3} s^2 (\Gamma - 1)\sqrt{\gamma\Omega_\phi}. \tag{19}$$

Equation (17) together with Eq. (19) encode the exact description of the dynamic evolution of the scalar field. In any case to find an exact solution it is a difficult task, and in order to proceed we consider two assumptions. First, we consider that the barotropic parameter of the scalar fluid is near to -1, therefore $\gamma \ll 1$. Second, we consider a near flat potential that is s is approximately constant, say $s \approx s_0$ [12].

In the limit $\gamma \ll 1$ we obtain from (18) an approximated equation with solution

$$\Omega_\phi(a) = [\beta(a^{-3(\alpha+1)} + \chi)^{\frac{1}{\alpha+1}} + 1]^{-1} \tag{20}$$

satisfying $\Omega_\phi(a = 1) = \Omega_{\phi 0}$, where

$$\beta = (1 - \Omega_{\phi 0})(\chi + 1)^{-\frac{1}{\alpha+1}} {\Omega_{\phi 0}}^{-1},$$

and $\chi = A/B$. Thus, in the limit $\chi \to 0$ is recovered the solution described by the expression (25) in Ref. [12]: $\Omega_\phi = [1 + (\Omega_{\phi 0}^{-1} - 1)a^{-3}]^{-1}$, corresponding to standard quintessence. From the solution (20) and from Eq. (8) we obtain the key formula

$$\omega_{\rm ch}(\Omega_\phi) = -\chi\beta^{\alpha+1}(1 - \Omega_\phi)^{-\alpha-1}\Omega_\phi^{\alpha+1}. \tag{21}$$

On the other hand, let us introduce the auxiliary function $\mu = \sqrt{\gamma}$. Assuming that Ω_ϕ is a monotonic function of the scale factor (in order to avoid that $d\Omega_\phi/da = 0$ at any value $a = a_0$), we obtain from (17) and (18)

$$\frac{d\mu}{d\Omega_\phi} = -\frac{(\mu^2 - 2)\left(3\mu - \sqrt{3} s_0 \sqrt{\Omega_\phi}\right)}{6(\Omega_\phi - 1)\Omega_\phi(-\mu^2 + \omega_{\rm ch} + 1)}, \tag{22}$$

where we have used the approximation $s \approx s_0 = \text{const}$. Using the hypothesis $\gamma \ll 1$ one is able to use the Taylor expansion of the above differential equation around $\mu = 0$ up to second order to obtain the approximated equation

$$\frac{d\mu}{d\Omega_\phi} = -\frac{s_0}{\sqrt{3}(\omega_{\rm ch} + 1)(\Omega_\phi - 1)\sqrt{\Omega_\phi}} + \frac{\mu}{(\omega_{\rm ch} + 1)(\Omega_\phi - 1)\Omega_\phi} + \mathcal{O}(\mu)^2. \tag{23}$$

Substituting into the Eq. (23) the expression $\omega_{\rm ch} = \omega_{\rm ch}(\Omega_\phi)$ given by (21) and integrating the resulting equation with the initial condition $\mu = 0$ at $\Omega_\phi = 0$ (which is true for the models we are considering here) we obtain the exact solution for $\alpha = 1$ given by

$$\mu(\Omega_\phi) = s_0 \mathcal{F}(\Omega_\phi)(F(\Omega|m) - E(\Omega|m)) + \frac{s_0\sqrt{\Omega_\phi}}{\sqrt{3}}, \tag{24}$$

where

$$\mathcal{F}(\Omega_\phi) = \frac{\sqrt{\Omega_\phi(\beta\sqrt{\chi} - 1) + 1}\sqrt{1 - \Omega_\phi(\beta\sqrt{\chi} + 1)}}{\Omega_\phi(\beta\sqrt{\chi} - 1)\sqrt{3\beta\sqrt{\chi} + 3}}, \tag{25}$$

$F(\Omega|m)$ and $E(\Omega|m)$ are the elliptic integral of the first and second kind respectively, with

$$\Omega = \sin^{-1}\left(\sqrt{\Omega_\phi}\sqrt{\beta\sqrt{\chi} + 1}\right), \tag{26}$$

and

$$m = \frac{2}{\beta\sqrt{\chi} + 1} - 1. \tag{27}$$

Finally we obtain the expression

$$1 + \omega = \mu(\Omega_\phi)^2. \tag{28}$$

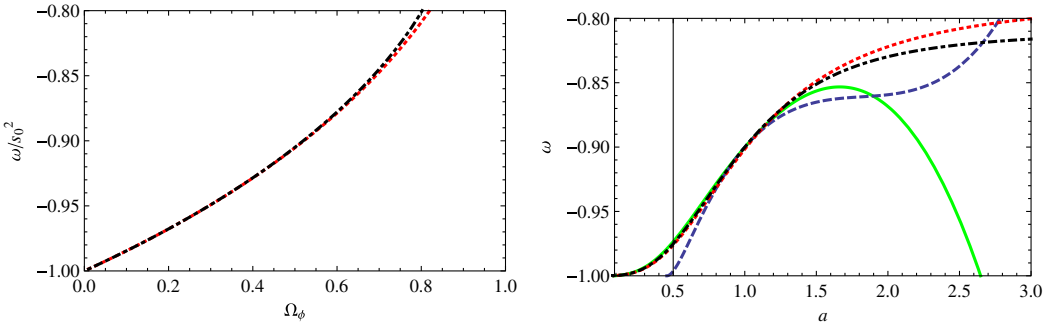

FIG. 1 (color online). (a) The value of ω/s_0^2 vs Ω_ϕ assuming a nearly flat potential and $\omega \sim -1$. The dotted (red) line corresponds to the approximated solution discovered in [12] (Eq. (23) in [12]) and the dash-dotted (dark) line corresponds to the approximated solution, (28), for $\chi = 0.1$, presented here. (b) EOS parameter of the scalar field for the exponential potential with slope $s_0 = 0.8029$. We have considered the initial conditions $\gamma(1) = 0.1$, $\Omega_\phi(1) = 0.7$, $s(1) = 0.8029$. The scale factor is normalized to 1 at present. The continuous (green) line corresponds to the exact value of $\omega(a)$ for model with solely a scalar field; the dashed (blue) line corresponds to the exact value of $\omega(a)$ for model that includes the Chaplygin gas; the dotted (red) line corresponds to the approximated solution found in [12] (Eq. (23) in [12]) and the dash-dotted (dark) line corresponds to the approximated solution, (28), presented here (assuming $\chi = 0.1$).

Expression (28) allows to obtain an exact solution for the dynamical evolutions of the barotropic index and using (20) we obtain $\omega = \omega(a)$. We would like to note that our solutions have the right dust limit when $A \to 0$ [12], this behavior is shown in Figs. 1(a) and 1(b).

In fact, in the limit $A \to 0$ (i.e., $\chi \to 0$), the deviation between our solution (28) and the solution (23) in [12] is given by the term

$$\frac{s_0^2(\Omega_\phi - 1)}{3\Omega_\phi^2} h(\Omega_\phi), \tag{29}$$

where

$$\begin{aligned} h(\Omega_\phi) = &\left(\sqrt{\Omega_\phi} - E\left(\sin^{-1}\left(\sqrt{\Omega_\phi}\right)\middle|1\right)\right)\left(\sqrt{\Omega_\phi}(\Omega_\phi + 1)\right. \\ &+ 2(\Omega_\phi - 1)\tanh^{-1}\left(\sqrt{\Omega_\phi}\right) \\ &\left. - (\Omega_\phi - 1)E\left(\sin^{-1}\left(\sqrt{\Omega_\phi}\right)\middle|1\right)\right). \end{aligned} \tag{30}$$

But

$$\begin{aligned} E(\Phi|m) &= \int_0^\Phi [1 - m\sin^2\theta]^{\frac{1}{2}} \mathrm{d}\theta \\ &= \int_0^{\sin\Phi} [1 - t^2]^{-\frac{1}{2}} [1 - mt^2]^{\frac{1}{2}} \mathrm{d}t. \end{aligned} \tag{31}$$

Thus,

$$\begin{aligned} E\left(\sin^{-1}\left(\sqrt{\Omega_\phi}\right)\middle|1\right) &= \int_0^{\sin^{-1}(\sqrt{\Omega_\phi})} [1 - \sin^2\theta]^{\frac{1}{2}} \mathrm{d}\theta \\ &= \int_0^{\sqrt{\Omega_\phi}} \mathrm{d}t = \sqrt{\Omega_\phi}. \end{aligned} \tag{32}$$

This means that $h(\Omega_\phi) \equiv 0$. That is, in the limit $A \to 0$, our solution (28) and the solution (23) in [12] coincides.

Particularly, in Fig. 1(a) depict the value of ω/s_0^2 vs Ω_ϕ assuming a nearly flat potential and $\omega \sim -1$. The dotted (red) line corresponds to the approximated solution discovered in [12] (Eq. (23) in [12]) and the dash-dotted (dark) line corresponds to the approximated solution, (28), for $\chi = 0.1$, presented here. In Fig. 1(b) the EOS parameter of the scalar field for the exponential potential with constant slope is displayed. The scale factor is normalized to 1 at present. The continuous (green) line corresponds to the exact value of $\omega(a)$ for model with solely a scalar field; the dashed (blue) line corresponds to the exact value of $\omega(a)$ for model with the addition of the Chaplygin gas; the dotted (red) line corresponds to the approximated solution discovered in [12] (Eq. (23) in [12]) and the dash-dotted (dark) line corresponds to the approximated solution, (28), presented here (assuming $\chi = 0.1$).

III. EXPONENTIAL POTENTIAL

In order to motivate the analysis for a general (arbitrary) potential, let us consider the simpler case of the exponential potential $V(\phi) = V_0 e^{-\lambda\phi}$ [34–45,47–54].

In order to do the analysis from the dynamical systems viewpoint of the mixture of a scalar field with exponential potential and a Chaplygin gas, we need to consider the variables x, y, s defined in the previous section plus the new variable

$$z = \frac{A}{3H^2\rho_{\mathrm{ch}}^\alpha}.$$

Then, from the equations of motions (1)–(3), we obtain the following autonomous system:

$$x' = -3x + \sqrt{\frac{3}{2}}\lambda y^2 + \frac{3}{2}x[1 + x^2 - y^2] - \frac{3}{2}xz,$$
$$y' = -\sqrt{\frac{3}{2}}\lambda xy + \frac{3}{2}y[1 + x^2 - y^2] - \frac{3}{2}yz, \quad (33)$$
$$z' = 3z[1 + \alpha + x^2 - y^2] - 3z^2 - \frac{3\alpha z^2}{1 - x^2 - y^2}.$$

We note, that in the dust limit ($A \to 0$) the variable z becomes automatically zero, the last equation in the system (33) is satisfied identically ($z = 0$ defines an invariant set) and the remaining Eqs. (33) correspond to the usual exponential quintessence scenario [34].

Now, it is convenient to express the observable magnitudes in terms of the phase space variables. These observable magnitudes are the dimensionless dark energy density, Ω_ϕ, given by (10), the equation of state (EOS) parameter of the dark energy given by

$$\omega \equiv \frac{P_\phi}{\rho_\phi} = \frac{x^2 - y^2}{x^2 + y^2}, \quad (34)$$

the EOS of the Chaplygin gas,

$$\omega_{\rm ch} \equiv \frac{P_{\rm ch}}{\rho_{\rm ch}} = -\frac{z}{1 - x^2 - y^2}, \quad (35)$$

the total (effective) EOS given by

$$\omega_{\rm tot} \equiv \frac{P_{\rm tot}}{\rho_{\rm tot}} = x^2 - y^2 - z, \quad (36)$$

and the deceleration parameter,

$$q \equiv -\frac{a\ddot{a}}{(\dot{a})^2} = -1 + \frac{3}{2}[1 + x^2 - y^2 - z]. \quad (37)$$

These expressions are valid not only at the fixed points but also they are valid in the whole phase space. Thus, we evaluate them at the fixed points in order to determine the type of solution that they represent.

In Table I we show the existence conditions for the real and physically meaningful (curves of) critical points of the autonomous system (33) associated to the exponential potential and also the values of the dark-energy density parameter $\Omega_{\rm DE}$, of the dark energy EOS parameter $\omega_{\rm DE}$, of the total EOS parameter $\omega_{\rm tot}$ and of the deceleration parameter q evaluated at them. In Table II the stability conditions for the critical points are presented.

Now, let us discuss in more details the stability conditions for the corresponding critical points. The critical point A associated to a matter dominated universe is a saddle point. Observe that the singular points B, C, D and F belong to the singular surface $x^2 + y^2 = 1$. In this case, both, the denominator and the numerator of Eq. (33) vanish simultaneously. In this case the additional eigenvalue due to the extra z coordinate could be finite positive or infinite with undefined sign depending of how the point is approached. Thus, linear approximation fails and we need to resort to numerical investigation. The critical points B and C, corresponding to stiff solutions, are always unstable. B (C resp.) is a local source for $\lambda > -\sqrt{6}$ ($\lambda < \sqrt{6}$, resp.), otherwise they are saddles. This argument is supported by numerical studies as shown in Figs. 2(a)–2(d) for the values of the parameters in the typical intervals (that are determined by the bifurcation values). Critical points D and E are the usual quintessence solutions widely investigated in the literature (see for instance [34]). Then, the main difference with respect to the results found in Ref. [34] is that, for $\alpha > 0$ none of them can be a late-time attractor. For D this argument is based on numerical analysis, since D belongs to the singular surface $x^2 + y^2$ and in this case, both the numerator and the denominator of the system (33) vanish, and then, the linear approximation is not valid. In the case of the point E we support this result in the fact that there exist one eigenvalues with positive real part. This means that if we include a GCG in the background, we cannot get a stable solution dominated by the scalar field (D) or an scaling solution (E). If we restrict our attention to the invariant set $z = 0$, then we have that D is a stable one for $\lambda^2 < 3$ and thus it can be the late-time state of the universe. In this case the equation for z is vanished identically, and we do

TABLE I. The real and physically meaningful critical points of the autonomous system (33) associated to the exponential potential. Stability conditions and the values of the dark energy density parameter $\Omega_{\rm DE}$, of the dark energy EOS parameter $\omega_{\rm DE}$, of the total EOS parameter $\omega_{\rm tot}$ and of the deceleration parameter q.

Label	x_c	y_c	z_c	Existence	Ω_ϕ	ω_ϕ	$\omega_{\rm ch}$	$\omega_{\rm tot}$	q
A	0	0	0	always	0	arbitrary	0	0	$\frac{1}{2}$
B	1	0	0	always	1	1	arbitrary	1	2
C	-1	0	0	always	1	1	arbitrary	1	2
D	$\frac{\lambda}{\sqrt{6}}$	$\sqrt{1 - \frac{\lambda^2}{6}}$	0	$\lambda^2 \leq 6$	1	$-1 + \frac{\lambda^2}{3}$	arbitrary	$-1 + \frac{\lambda^2}{3}$	$-1 + \frac{\lambda^2}{2}$
E	$\sqrt{\frac{3}{2}}\frac{1}{\lambda}$	$\sqrt{\frac{3}{2(\lambda)^2}}$	0	$\lambda^2 \geq 3$	$\frac{3}{\lambda^2}$	0	0	0	$\frac{1}{2}$
F	0	1	0	$\lambda = 0$	1	-1	arbitrary	-1	-1
G	0	y_c	$1 - y_c^2$	$y_c^2 < 1$, $y_c \neq 0$, $\lambda = 0$	y_c^2	-1	-1	-1	-1
K	0	0	1	always	0	arbitrary	-1	-1	-1

TABLE II. The real and physically meaningful critical points of the autonomous system (33) associated to the exponential potential. Stability conditions, NH stands for nonhyperbolic. Observe that the critical points B, C, D and F belong to the singular surface $x^2 + y^2 = 1$. In this case both denominator and numerator of (33) vanish simultaneously. In this case the additional eigenvalue due to the extra z coordinate could be finite positive or infinite with undefined sign depending of how the point is approached. Thus, linear approximation fails and we need to resort to numerical investigation.

Label	Eigenvalues	Stability
A	$-\frac{3}{2}, \frac{3}{2}, 3(1+\alpha)$	saddle
B	$3, 3-\sqrt{\frac{3}{2}}\lambda$, undef.	unstable
C	$3, 3+\sqrt{\frac{3}{2}}\lambda$, undef.	unstable
D	$-3+\lambda^2, -\frac{1}{2}(6-\lambda^2)$, undef.	saddle
E	$3(1+\alpha), \beta^-, \beta^+$	saddle
F	$-3, -3$, undef.	stable (see Appendix A)
G	$0, -3(1+\alpha), -3$	NH
K	$-3, 0, -3(1+\alpha)$	stable

not require to include this variable in the analysis. D corresponds to a dark-energy-dominated universe, with a dark energy EOS in the quintessence regime, which can be accelerating or not according to the λ value. Additionally, this solution is free of instabilities. This point is quite important, since it is stable and possesses ω_{DE} and q compatible with observations [34]. Point E is stable in the invariant set $z = 0$. It can attract the universe at late times (in case of a GCG behaving as dust), and it is free of instabilities. It has the advantage that the dark energy density parameter lies in the interval $0 < \Omega_{\mathrm{DE}} < 1$, that is it can alleviate the coincidence problem, but it has the disadvantage that it is not accelerating and possesses $\omega_{\mathrm{DE}} = 0$, which are not favored by observations [34]. However, let us remark that they are saddles for the full vector field. The solution F exists for $\lambda = 0$. It represents a de Sitter solution which is stable but not asymptotically stable (see Appendix A 1). The curve of critical points G (which exists only for $\lambda = 0$) is stable but not asymptotically stable, whereas, K is asymptotically stable (see details of the center manifold calculations for both G and K in Appendix B). To finish this section let us proceed to a discussion of the following numerical elaborations:

(i) Figure 2(a) shows several orbits for the values of the parameters $\alpha = 0.5$, $\lambda = 0$. B and C are local sources; A is a saddle. F coincides with D (contained in the curve G) and it is stable but not asymptotically stable for $f(0) \geq 0$, otherwise it is a saddle (see Appendix A 2). E does not exist. Any arbitrary point in the curve G (that exist only for $\lambda = 0$) is stable, attracting an open set of orbits. The center manifold of K is stable.

(ii) In Fig. 2(b) we presented several orbits in the phase space for $\alpha = 0.5$, $\lambda = 1$. The kinetic-dominated solutions B and C are local sources, the matter-dominated solution A and the scalar-field-dominated solution D are saddles, and the Chaplygin-gas-dominated solutions (which also mimic a de Sitter solution) K is the attractor. D is a local attractor in the invariant set $z = 0$.

(iii) Figure 2(c) shows several orbits in the phase space for $\alpha = 0.5$, $\lambda = 2$. B and C are local sources, A, D and E are saddles, and K is the attractor. E is a local attractor in the invariant set $z = 0$.

(iv) Finally, in Fig. 2(d) we display several orbits in the phase space for $\alpha = 0.5$, $\lambda = 3$. B (the kinetic-dominated solution with $\lambda x > 0$) is a saddle point, C (the kinetic-dominated solution with $\lambda x > 0$) is the local source (unstable node), D does not exist, A and E are saddles, and K is the attractor. E is a local (spiral) attractor in the invariant set $z = 0$.

Now, as commented before, it is a fact that the dynamical evolution leave the coordinates (x, y) within the upper-half unit disc. However, the only restriction on z is that $z \geq 0$. This means that in principle the z coordinate could be unbounded and, then, there might exist critical points at infinity (which would correspond to $z \to +\infty$). In order to determine the fixed points at infinity and study their stability, we need to compactify the phase space using the Poincaré method. Transforming to polar coordinates $(r(\tau), \theta(\tau), \psi(\tau))$ [69–71],

$$x = r\cos\theta\sin\psi, \quad y = r\cos\theta\sin\psi, \quad z = r\cos\psi, \tag{38}$$

where $0 \leq \psi \leq \frac{\pi}{2}$, $0 \leq \theta \leq \pi$ and substituting $r = \frac{R}{1-R}$, the regime $r \to \infty$ corresponds to $R \to 1$. The points x, y, z are mapped onto

$$x_R = R\cos\theta\sin\psi, \quad y_R = R\cos\theta\sin\psi, \quad z_R = R\cos\psi; \tag{39}$$

thus, the points at infinity are mapped on the unitary sphere $R = 1$.

Using this coordinate transformation, introducing the new time variable $d\eta = \frac{d\tau}{(1-R)}$, which preserves the time orientation, the leading terms of the system (33) as $R \to 1$ are

$$R' \to \frac{3(\cos(2\theta)(\cos(2\psi) + 3)\sin^2\psi)}{4}, \tag{40}$$

$$\theta' \to -\sqrt{\frac{3}{2}}\lambda\sin\theta\sin\psi, \tag{41}$$

$$\psi' \to -\frac{3(\cos(2\theta)\cos\psi\sin^3\psi)}{2(1-R)}, \tag{42}$$

where now the comma denotes the derivative with respect to η. In this case the radial equation does not contain the radial coordinate; thus, the fixed points can be obtained using just the angular equations. Setting $\theta' = 0$ and $\psi' = 0$, we obtain that the fixed point with

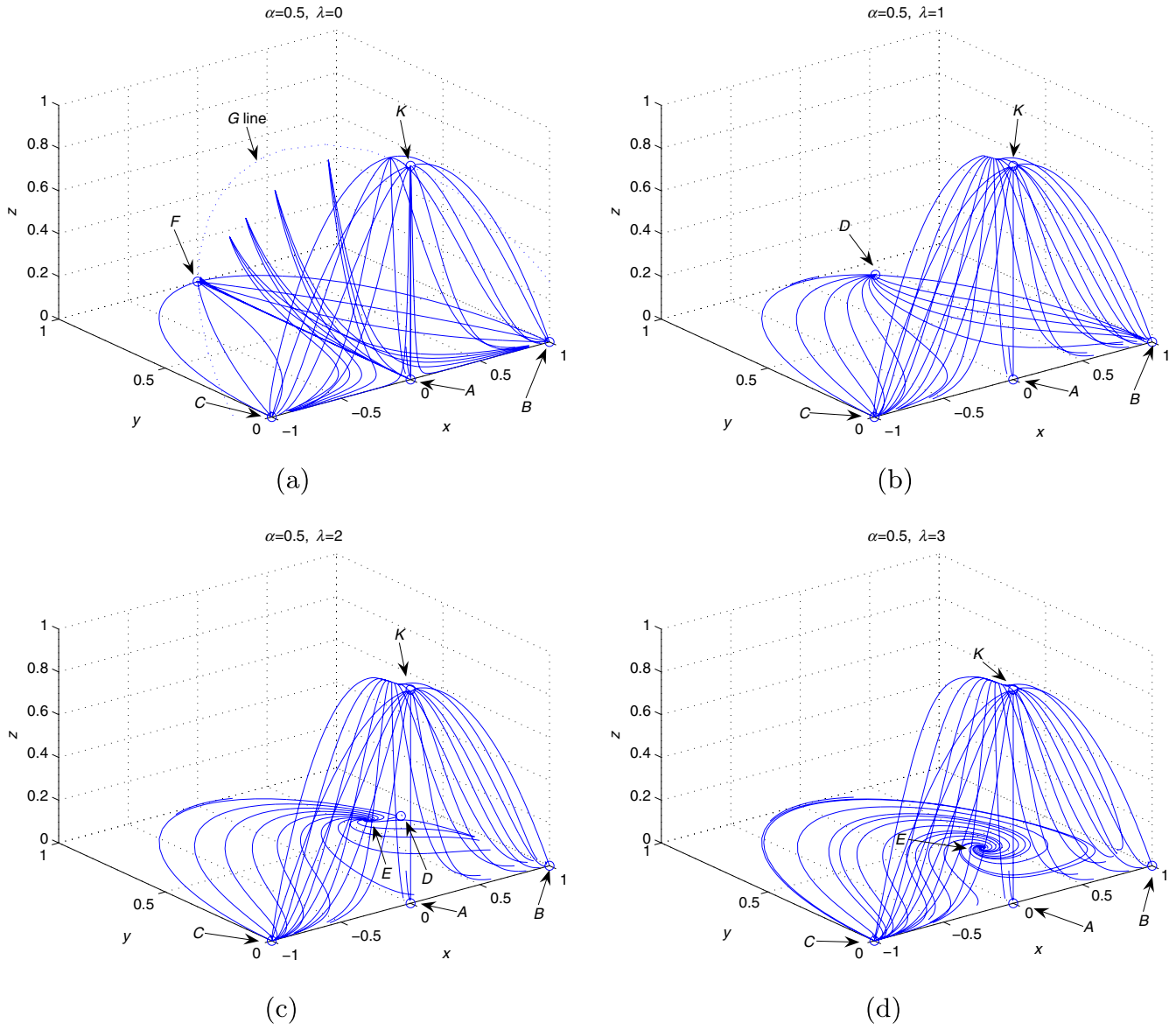

FIG. 2 (color online). The phase space of the system (33). Without lack of generality we use $\alpha = 0.5$. (a) $\lambda = 0$. B and C are local sources; A is a saddle. F coincides with D (contained in the curve G) and it is stable but not asymptotically stable for $f(0) \geq 0$; otherwise, it is a saddle (see Appendix A 2). E does not exist. Any arbitrary point in the curve G (that exists only for $\lambda = 0$) is stable, attracting an open set of orbits. The center manifold of K is stable, as is K. (b) $\lambda = 1$. B and C are local sources; A and D are saddles and K is the attractor. D is a local attractor in the invariant set $z = 0$. The solutions at the x-y plane correspond to those in Fig. 2 in [34]. (c) $\lambda = 2$. B and C are local sources; A, D, and E are saddles, and K is the attractor. E is a local attractor in the invariant set $z = 0$. The solutions at the x-y plane correspond to those in Fig. 3 in [34]. (d) $\lambda = 3$. B (the kinetic-dominated solution with $\lambda x > 0$) is a saddle point, C (the kinetic-dominated solution with $\lambda x < 0$) is the local source (unstable node), D does not exist, A and E are saddles, and K is the attractor. E is a local (spiral) attractor in the invariant set $z = 0$. The solutions at the x-y plane correspond to those in Fig. 4 in [34].

physical sense ($0 \leq \Omega_\phi \leq 1$) must satisfy $\psi = 0$, i.e., $(x_R, y_R, z_R) = (0, 0, 1)$. In this case the eigenvalues of the Jacobian matrix associated with the angular coordinates are $\{0, 0\}$ and $R' = 0$ at the equilibrium point. Then, we cannot obtain information on their stability using the linearization. The complete analysis is outside the scope of the present investigation.

IV. PHASE-SPACE ANALYSIS WITHOUT POTENTIAL SPECIFICATION

In order to transform the system (12)–(14) to an autonomous one, first it is necessary to determine a specific potential form $V(\phi)$ of the scalar field ϕ. However, using the above example as a motivation, one could alternatively

handle the potential differentiations using the auxiliary variable s given by

$$s = -\frac{V'(\phi)}{V(\phi)}, \tag{43}$$

while keeping the potential still arbitrary.[1] The next step is to introduce the function

$$f \equiv s^2(\Gamma - 1) = \frac{V''(\phi)}{V(\phi)} - \frac{V'(\phi)^2}{V(\phi)^2} \tag{44}$$

as an arbitrary function of s. In fact, if f can be expressed as an explicit one-valued function of s, that is $f = f(s)$, then, it is possible to write a closed dynamical system for s and a set of normalized variables. On the other hand, by giving $f(s)$, nonidentically equal to zero, we obtain the expressions

$$\phi(s) = \phi_0 - \int_{s_0}^{s} \frac{1}{f(K)}\, dK, \tag{45}$$

$$V(s) = e^{\int_{s_0}^{s} \frac{K}{f(K)} dK} \bar{V}_0, \tag{46}$$

where the integration constants satisfy $V(s_0) = \bar{V}_0$, $\phi(s_0) = \phi_0$.[2] Thus, it is possible to reconstruct the potential V by the elimination of s between (45) and (46). For the usual cosmological cases the potential can be written explicitly, that is $V = V(\phi)$. The details of the method, coined "Method of f-devisers", were presented in [55]. This method has the significant advantage, that one can first perform the analysis for arbitrary potentials and then just substitute the desired forms, instead of repeating the whole procedure for every distinct potential (see [55] and references therein).

Then, from the equations of motions (1)–(3) we get the following autonomous system:

$$\begin{aligned} x' &= -3x + \sqrt{\frac{3}{2}} s y^2 + \frac{3}{2} x[1 + x^2 - y^2] - \frac{3}{2} x z, \\ y' &= -\sqrt{\frac{3}{2}} s x y + \frac{3}{2} y[1 + x^2 - y^2] - \frac{3}{2} y z, \\ z' &= 3z[1 + \alpha + x^2 - y^2] - 3z^2 - \frac{3\alpha z^2}{1 - x^2 - y^2}, \\ s' &= -\sqrt{6} f(s) x. \end{aligned} \tag{47}$$

In Table III we present the existence conditions for the real and physically meaningful (curves of) critical points of the autonomous system (47). We use the notation s^* for the values of $s = s^*$ such that $f(s^*) = 0$, and s_c for denoting arbitrary values of s at equilibrium. We display also the corresponding values of the dark energy density parameter Ω_ϕ, of the dark energy EOS parameter ω_ϕ, of the EOS of Chaplygin gas $\omega_{\rm ch}$, of the total EOS $\omega_{\rm tot}$ and of the deceleration parameter q. In Table IV the stability conditions for the critical points are presented.

Now, let us comment briefly on the stability and physical interpretation of the critical points of (47).

The curve of critical point A is always a saddle. It represents cosmological solutions dominated by the Chaplygin gas mimicking dust, this solution correlates with the transient matter dominated epoch of the universe. Observe that the critical points $B(s^*)$, $C(s^*)$, $D(s^*)$ with s^* such that $f(s^*) = 0$ and F belong to the singular surface $x^2 + y^2 = 1$. In this case both denominator and numerator of (47) are vanished simultaneously. In this case the additional eigenvalue due to the extra z coordinate could be finite positive or infinite with undefined sign depending of how the point is approached. For F there are two eigenvalues whose nature depends on the way that F is approached, for that reason they are undefined.

For s^*, the solutions $B(s^*)$ and $C(s^*)$ are past attractors or saddle points under the same conditions of the standard quintessence scenario [34] with the identification $s^* \equiv \lambda$ (see Table IV). They represent solutions dominated by the kinetic energy of the scalar field mimicking a stiff fluid. The solutions $D(s^*)$, $E(s^*)$ and F represents the scalar-field- dominated solution, the matter-scalar scaling solution, and de Sitter solutions dominated by the potential energy of the scalar field, respectively. The main difference here with respect the standard quintessence scenario [34] is that $D(s^*)$, $E(s^*)$ are saddle points (we are considering $\alpha > 0$). So, the standard quintessence solutions are not late-time solutions in this scenario. For analyzing the important critical point F, the linear approximation fails and we need to resort to numerical studies or include higher order terms in the analysis. In fact, following our approach in Appendix A 2, we find that actually F is the late-time attractor for $f(0) > 0$ and a saddle for $f(0) < 0$.

Combining expressions (16) and (35) we find that as $\tau \to +\infty$, $z \to 1 - x^2 - y^2$. Thus at late times we can approximate the system (47) by

$$x' = -3x + 3x^3 + \sqrt{\frac{3}{2}} s y^2, \qquad y' = -\sqrt{\frac{3}{2}} s x y + 3 y x^2, \qquad s' = -\sqrt{6} f(s) x, \tag{48}$$

and the decoupled equation

$$z' = 6 z x^2. \tag{49}$$

If $x \to x_c \neq 0$ as $\tau \to +\infty$, then from Eq. (49) follows that z increases without bound in contradiction with the boundedness of $1 - x^2 - y^2$. Thus, as time goes forward, $x \to 0$. Hence $z \to 1 - y_c^2$ where $0 \leq y_c \leq 1$. By calculating the critical points of the system (48) and analyzing their linear

[1] The variable s is just a constant ($s \equiv \lambda$) for the exponential potential $V = V_0 e^{-\lambda\phi}$.

[2] We would like to note that due the requirement that f must be different to zero this procedure cannot be applied to the case of the exponential potential for which f vanishes identically. For this reason we studied the exponential potential in the previous section separately.

TABLE III. The real and physically meaningful (curves of) critical points of the autonomous system (47). Existence conditions and the values of the dark energy density parameter $\Omega_{\rm DE}$, of the dark energy EOS parameter $\omega_{\rm DE}$, of the total EOS parameter $\omega_{\rm tot}$ and of the deceleration parameter q. We use the notation s^* for the values of $s = s^*$ such that $f(s^*) = 0$, and s_c for denoting arbitrary values of s at equilibrium.

Label	x_c	y_c	z_c	s_c	Existence	Ω_ϕ	ω_ϕ	$\omega_{\rm ch}$	$\omega_{\rm tot}$	q
A	0	0	0	s_c	always	0	arbitrary	0	0	$\frac{1}{2}$
$B(s^*)$	1	0	0	s^*	always	1	1	arbitrary	1	2
$C(s^*)$	-1	0	0	s^*	always	1	1	arbitrary	1	2
$D(s^*)$	$\frac{s^*}{\sqrt{6}}$	$\sqrt{1-\frac{(s^*)^2}{6}}$	0	s^*	$(s^*)^2 \leq 6$	1	$-1+\frac{(s^*)^2}{3}$	arbitrary	$-1+\frac{(s^*)^2}{3}$	$-1+\frac{(s^*)^2}{2}$
$E(s^*)$	$\sqrt{\frac{3}{2}}\frac{1}{s^*}$	$\sqrt{\frac{3}{2(s^*)^2}}$	0	s^*	$(s^*)^2 \geq 3$	$\frac{3}{(s^*)^2}$	0	0	0	$\frac{1}{2}$
F	0	1	0	0	always	1	-1	arbitrary	-1	-1
G	0	y_c	$1-y_c^2$	0	$y_c^2 < 1$, $y_c \neq 0$	y_c^2	-1	-1	-1	-1
K	0	0	1	s_c	always	0	arbitrary	-1	-1	-1

TABLE IV. The real and physically meaningful critical points of the autonomous system (47). Stability conditions, NH stands for nonhyperbolic. We introduce the notations $\beta^\pm(s^*) = \frac{3}{4}(-1 \pm \frac{\sqrt{24(s^*)^2-7(s^*)^4}}{(s^*)^2})$, $\delta^\pm = -\frac{3}{2}(1 \pm \sqrt{1-\frac{4}{3}f(0)})$, and $\Delta^\pm = -\frac{3}{2}(1 \pm \sqrt{1-\frac{4}{3}y_c^2 f(0)})$. Observe that the critical points $B(s^*)$, $C(s^*)$, $D(s^*)$ and F belong to the singular surface $x^2 + y^2 = 1$. In this case both denominator and numerator of (47) are vanished simultaneously. In this case the additional eigenvalue due to the extra z coordinate could be finite positive or infinite with undefined sign depending of how the point is approached. For F there are two eigenvalues whose nature depends on the way that F is approached. For that reason they are undefined. Thus, linear approximation fails and we need to resort to numerical works.

Label	Eigenvalues	Stability
A	$-\frac{3}{2}, \frac{3}{2}, 0, 3(1+\alpha)$	saddle
$B(s^*)$	$3, 3-\sqrt{\frac{3}{2}}s^*, -\sqrt{6}f'(s^*)$, undef.	unstable
$C(s^*)$	$3, 3+\sqrt{\frac{3}{2}}s^*, \sqrt{6}f'(s^*)$, undef.	unstable
$D(s^*)$	$-3+(s^*)^2, -\frac{1}{2}(6-(s^*)^2), -s^*f'(s^*)$, undef.	saddle
$E(s^*)$	$3(1+\alpha), \beta^-(s^*), \beta^+(s^*), -\frac{3f'(s^*)}{s^*}$	saddle
F	undef., undef., δ^+, δ^-	stable (see Appendix A 2)
G	$0, -3(1+\alpha), -3, \Delta^+, \Delta^-$	NH, stable for $f(0) > 0$, $y_c > 0$, saddle otherwise
K	$-3, 0, 0, -3(1+\alpha)$	NH (unstable)

stability we find that the only candidates to be the late-time attractors are

(i) the curve G which has the following system of eigenvalues and eigenvectors:

$$\begin{pmatrix} 0, & \Delta^+, & \Delta^- \\ \{0,1,0\}, & \left\{-\frac{\Delta^+}{\sqrt{6}f(0)}, 0, 1\right\}, & \left\{-\frac{\Delta^-}{\sqrt{6}f(0)}, 0, 1\right\} \end{pmatrix},$$

where $\Delta^\pm = -\frac{3}{2}(1 \pm \sqrt{1-\frac{4}{3}y_c^2 f(0)})$. Since the center subspace is tangent to the y axis, follows that the curve is normally hyperbolic.[3] Then follows the stability of G on the space (x, y, s). This argument is not complete, since we have forgotten about what happens in the z direction. In fact, in the general case (when the z direction is included in the analysis), this curve is actually nonhyperbolic and it is not normally hyperbolic anymore, thus we cannot obtain information about its stability looking at the linearization. This one is the main difference that appears when considering the extra direction z.

(ii) The other candidate is the curve K which have the following system of eigenvalues and eigenvectors

$$\begin{pmatrix} -3, & 0, & 0 \\ \left\{\frac{\sqrt{\frac{3}{2}}}{f(s_c)}, 0, 1\right\}, & \{0,0,1\}, & \{0,1,0\} \end{pmatrix},$$

which is also normally hyperbolic (the center subspace is the plane y-s is tangent to the line $s = s_c$).

[3]Recall that a set of nonisolated critical points is said to be normally hyperbolic if the only eigenvalues with zero real parts are those whose corresponding eigenvectors are tangent to the set. In this case the stability of the set can be deduced by examining the signs of the remaining non-null eigenvalues (i.e., for a curve, in the remaining $n-1$ directions) [72].

(iii) Finally, both numerical simulations and analytical methods suggest that F (contained in the curve G) is an attractor for $f(0) > 0$, and for $f(0) < 0$, it is a saddle (see Appendix A 2).

The above heuristic reasoning suggests that the future attractor of the system (47) is located at the curve G, which contains the especial point F, or it is located at the curve K.

With the exception of the point F, which is dominated by a constant potential, G represents a class of solutions where neither the potential energy of the scalar field nor the Chaplygin gas dominates. On the other hand, the curve K corresponds to purely Chaplygin-gas-dominated solutions (which also mimic a de Sitter solution).

Indeed, using the center manifold theory, it can be proven that if the condition $f(0) > 0$ is satisfied, the curve of fixed points G is stable but not asymptotically stable. Applying the same procedure to the curve K, we find that also the curve K is stable but not asymptotically stable. The details of the calculation are presented in Appendix C.

To investigate the dynamics at infinity, one introduces the Poincaré variables [69–71]

$$x = \frac{R}{1-R}\cos\theta\sin\varphi\sin\psi, \quad y = \frac{R}{1-R}\sin\theta\sin\varphi\sin\psi,$$
$$z = \frac{R}{1-R}\sin\varphi\cos\psi, \quad s = \frac{R}{1-R}\cos\varphi, \tag{50}$$

where $0 \leq \psi \leq \frac{\pi}{2}$, $0 \leq \theta \leq \pi$ and $0 \leq \varphi \leq \pi$, and the new time variable $d\eta = \frac{d\tau}{(1-R)}$, which preserves the time orientation. The region at infinity $x^2 + y^2 + z^2 + s^2 \to \infty$

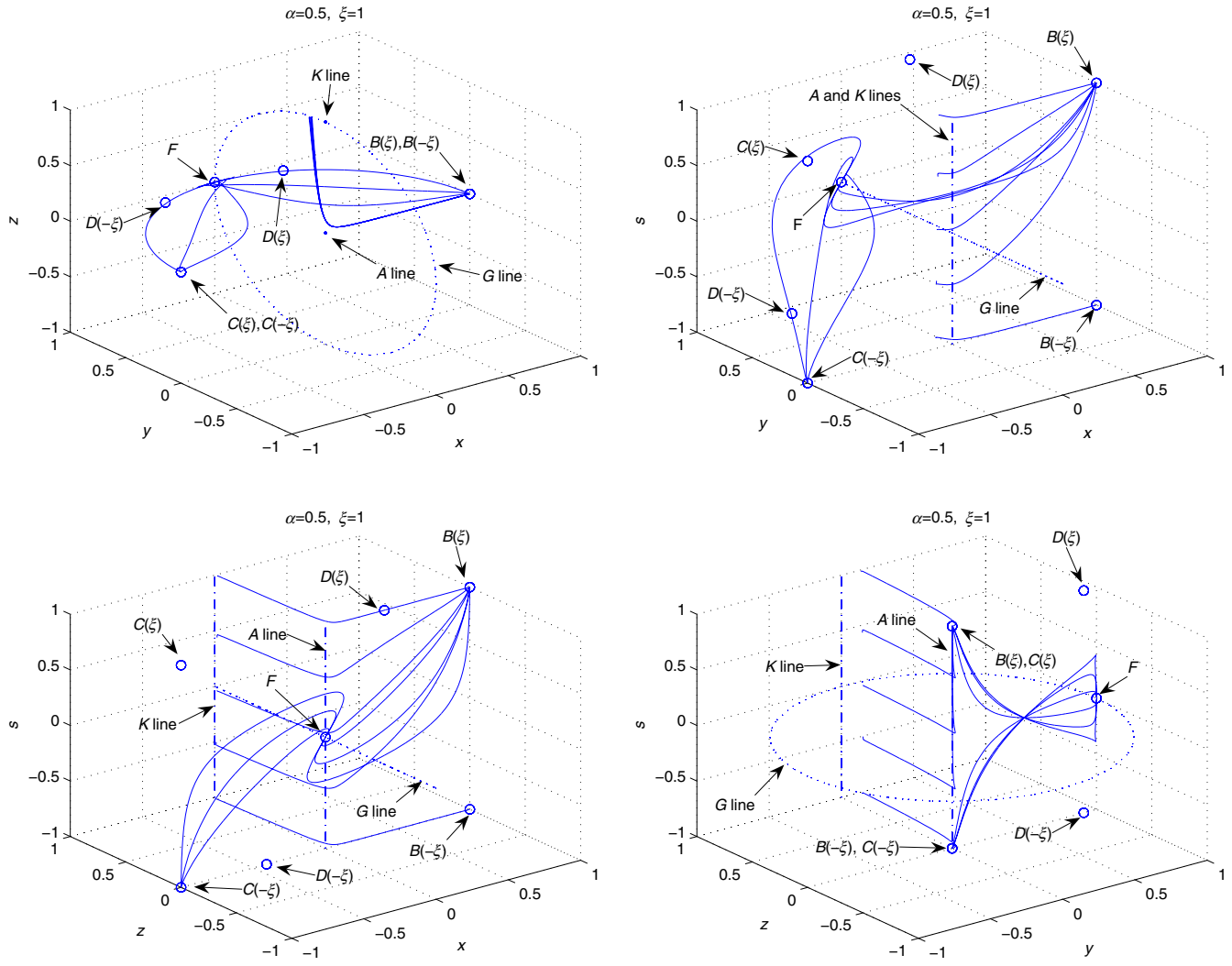

FIG. 3 (color online). Projections of some orbits in the phase space of the system (47) for $\xi = 1$. Without lack of generality we use $\alpha = 0.5$. Observe that $B(\pm\xi)$ and $C(\pm\xi)$ are local sources and the point F located at the curve G is a local attractor. The curve K is stable, but not asymptotically stable. The scalar-field-dominated solution $D(\pm\xi)$ are of the saddle type, as well as the rest of the (curves of) fixed points. The scaling solutions $E(\pm\xi)$ do not exist.

corresponds to the region $R \longrightarrow 1$ in the R, θ, φ, ψ space. Then, we take the limit $R \longrightarrow 1$ in R', θ', φ', ψ', where now the comma denotes the derivative with respect to η, and preserve the leading terms. In the case that the radial equation does not contain the radial coordinate, the fixed points can be obtained using just the angular equations. Setting $\theta' = 0$, $\psi' = 0$ and $\varphi' = 0$, are obtained as the fixed points. The stability of these points is studied by analyzing first the stability of the angular coordinates and then deducing, from the sign of R', the stability on the radial direction [69–71]. That is, it is required $R' > 0$ at equilibrium. This means that the radial coordinate increases in value until reaching the boundary $R = 1$ from below. To do the analysis, it is required to provide the functional form of $f(s)$; however, the complete analysis is outside the scope of the present paper.

A. An example: coshlike potential

The coshlike potential $V(\phi) = V_0[\cosh(\xi\phi) - 1]$ has been widely studied in the literature (see, for example, [50,54,55,57,58,73–78]). For this potential,

$$f(s) = -\frac{1}{2}(s - \xi)(s + \xi). \tag{51}$$

Observe that $f(0) = \frac{1}{2}\xi^2 > 0$. This is the sufficient condition for the stability of the class of de Sitter solutions represented by the curve of critical points G. For this choice $s^* \in \{\xi, -\xi\}$. Also $f'(s) = -s$, thus $f'(\xi) = -\xi$, $f'(-\xi) = \xi$. For this choice the system (47) admits twelve (curves of) critical points denoted by A, $B(\xi)$, $B(-\xi)$, $C(\xi)$, $C(-\xi)$, $D(\xi)$, $D(-\xi)$, $E(\xi)$, $E(-\xi)$, F, G and K.

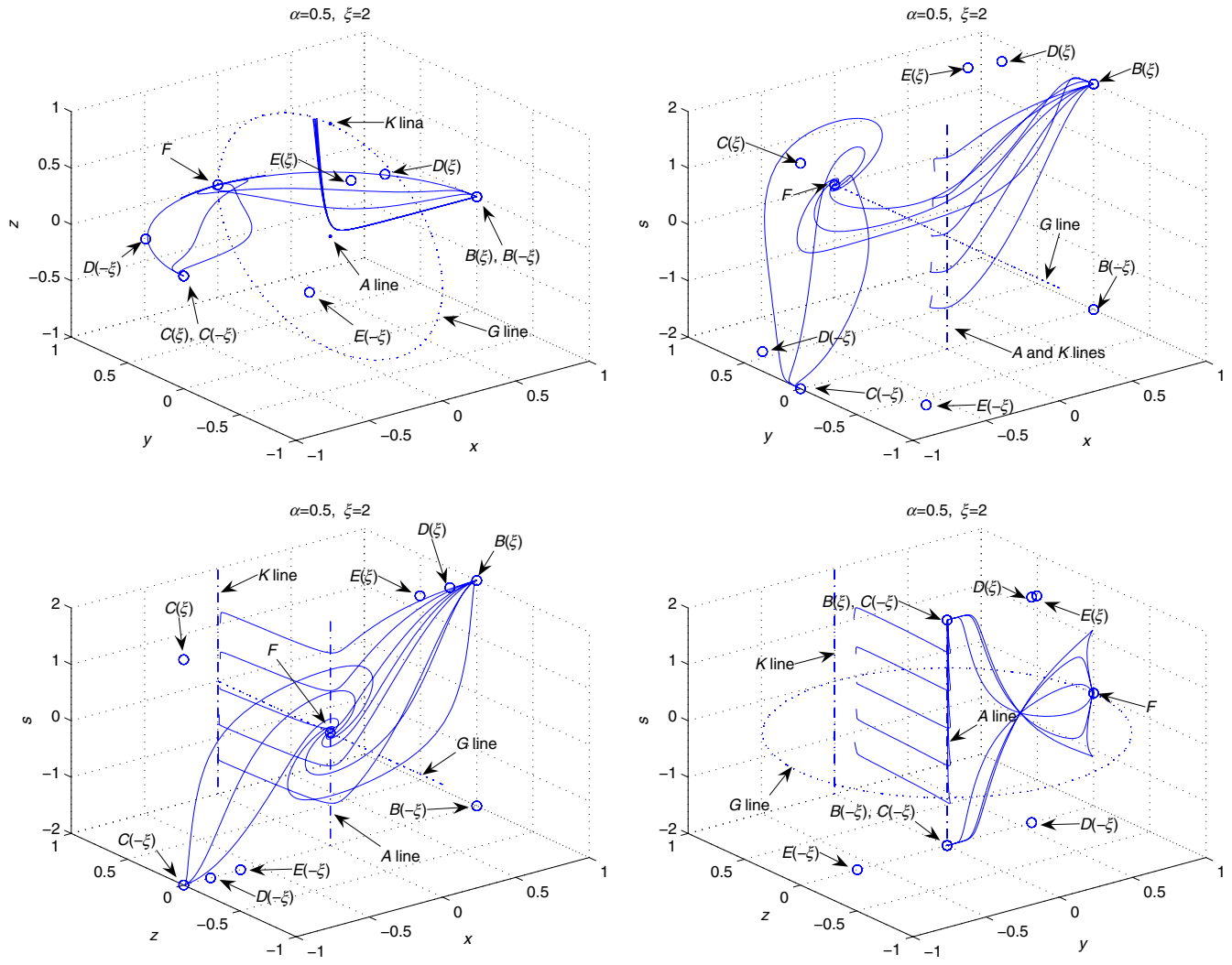

FIG. 4 (color online). Projections of some orbits in the phase space of the system (47) for $\xi = 2$. Without lack of generality we use $\alpha = 0.5$. Note that $B(\pm\xi)$ and $C(\pm\xi)$ are local sources and the point F located at the curve G is a local attractor. The curve K is stable, but not asymptotically stable. The scalar-field-dominated solution $D(\pm\xi)$ and the scaling solution $E(\pm\xi)$ are of the saddle type, as well as the rest of the (curves of) fixed points.

To finish this section, let us discuss the following numerical simulations:

(i) In Fig. 3 are displayed the projections of some orbits in the phase space of the system (47) for $\alpha = 0.5$, $\xi = 1$. $B(\pm\xi)$ and $C(\pm\xi)$ are local sources and the point F located at the curve G is a local attractor. The curve K is stable, but not asymptotically stable. The scalar-field-dominated solution $D(\pm\xi)$ are of the saddle type, as well as the rest of the (curves of) fixed points. The scaling solutions $E(\pm\xi)$ do not exist.

(ii) In Fig. 4 some projections are displayed of orbits in the phase space of the system (47) for $\alpha = 0.5$, $\xi = 2$. Note that $B(\pm\xi)$ and $C(\pm\xi)$ are local sources and the point F located at the curve G is a local attractor. The curve K is stable, but not asymptotically stable. The scalar-field-dominated solution $D(\pm\xi)$ and the scaling solution $E(\pm\xi)$ are of the saddle type, as well as the rest of the (curves of) fixed points.

(iii) In Fig. 5 are presented the projections of some orbits in the phase space of the system (47) for $\alpha = 0.5$, $\xi = 3$. Observe that $B(\pm\xi)$ and $C(\pm\xi)$ are local sources and the point F located at the curve G is a local attractor. The curve K is stable, but not asymptotically stable. The scalar-field-dominated solution $D(\pm\xi)$ and the scaling solution $E(\pm\xi)$ are of the saddle type, as well as the rest of the (curves of) fixed points.

Summarizing, for arbitrary potentials, using the numerical simulations to support our conjectures, and employing analytical tools as the main proof, we have corroborated

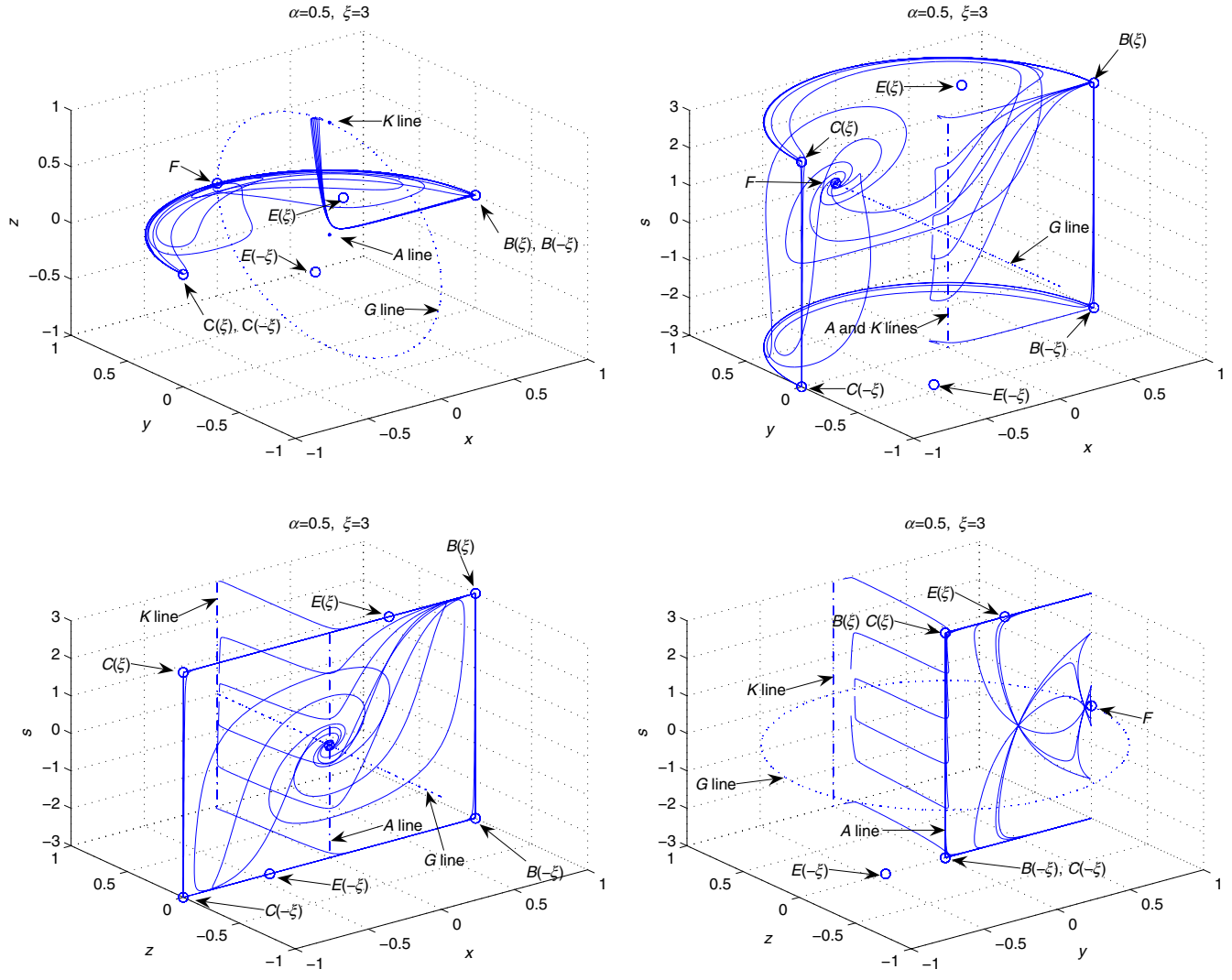

FIG. 5 (color online). Projections of some orbits in the phase space of the system (47) for $\xi = 3$. Without lack of generality we use $\alpha = 0.5$. $B(\pm\xi)$ and $C(\pm\xi)$ are local sources and the point F located at the curve G is a local attractor. The curve K is stable, but not asymptotically stable. The scalar-field-dominated solution $D(\pm\xi)$ and the scaling solution $E(\pm\xi)$ are of the saddle type, as well as the rest of the (curves of) fixed points.

that F is a late-time attractor, which is contained in the curve G. The curve of fixed points G and K are stable but not asymptotically stable. The numerical simulations suggest that the early time attractors are

(i) $B(\xi)$ or $C(-\xi)$ for $0 < \xi < \sqrt{6}$;
(ii) $B(-\xi)$ or $C(\xi)$ for $-\sqrt{6} < \xi < 0$.

The rest of the (curves of) critical points are saddle points.

V. FINAL REMARKS

In the present work we have studied the thawing dark energy scenarios with the Chaplygin gas as the other matter content of the universe and different kinds of self-interacting potentials for the scalar field. First, we obtain the exact solution for the cosmological equation of our model in terms of the elliptic function of the first and second kind, and we obtain the right limit in the case of dust matter. Second, we used the cosmological model for the exponential potential for the scalar field, and also we perform the dynamical systems analysis and we characterize the phase space of this system. We found the critical point of this system and studied the stability of this point. The main characteristics of this phase space are

(i) The critical point A is always a saddle. It represents cosmological solutions dominated by the Chaplygin gas mimicking dust, this solution correlates with the transient matter dominated epoch of the universe.
(ii) The critical points B and C corresponding to stiff solutions are always unstable. B (C resp.) is a local source for $\lambda > -\sqrt{6}$ ($\lambda < \sqrt{6}$, resp.); otherwise, they are saddles.
(iii) The usual quintessence points D (scalar-field-dominated solution) and E (the usual scaling scalar field matter solution) [34] cannot be the late-time attractors due to the presence of a GCG with $\alpha > 0$ in the background. However, in the limit $A \to 0$, when the Chaplygin gas behaves as dust and the z variable is not required, we recover the standard quintessence scenario [34]. This is a crucial difference with respect to previous works in the literature.
(iv) For a constant potential (exponential with $\lambda = 0$), the solution F represents a de Sitter solution that is stable but not asymptotically stable (see Appendix A 1).
(v) For a constant potential (exponential with $\lambda = 0$), the curve of critical points G is stable but not asymptotically stable (see details in Appendix B).
(vi) For an exponential potential ($\lambda \neq 0$), K is asymptotically stable (see details in Appendix B).

Finally for analyzing general potential $V(\phi)$ we used the "Method of f-devisers" and we obtained the critical point for this dynamical system and also we characterized the phase space and we studied the stability of the critical point. In this case, the principal characteristic of this phase space are

(i) For arbitrary potentials, the curve of critical points A, representing dust solutions, is always a saddle. This solution correlated with the transient-matter-dominated epoch of the universe.
(ii) Considering s^* such that $f(s^*) = 0$. For these s values, the solutions $B(s^*)$ and $C(s^*)$ are past attractors or saddle points under the same conditions of the standard quintessence scenario [34] with the identification $s^* \equiv \lambda$ (see Table IV).
(iii) For the same s values, the standard quintessence solutions $D(s^*)$, $E(s^*)$ are saddle points (we are considering $\alpha > 0$). This is the main difference here with respect the results for the standard quintessence scenario [34]. In the dust limit $A \to 0$, the standard quintessence scenario is recovered [34] since the z variable is not required anymore in the dynamics.
(iv) For arbitrary potentials and provided $f(0) > 0$, F (contained in the curve G) is an attractor and for $f(0) < 0$, it is a saddle (see Appendix A 2).
(v) For arbitrary potentials and provided $f(0) > 0$, the curve of fixed points G is stable but not asymptotically stable (see Appendix C).
(vi) For arbitrary potentials, the curve K is stable but not asymptotically stable (see Appendix C).

ACKNOWLEDGMENTS

This work was funded by Comisión Nacional de Ciencias y Tecnología through FONDECYT Grants No. 1110230 (S. d. C. and R. H.), No. 1130628 (R. H. and S. d. C.), and No. 1110076 (S. d. C. and J. S.) and by DI-PUCV Grants No. 123710 (S. d. C.), No. 123724 (R. H.), and No. 123713 (J. S.). C. L. was supported by Grant No. UTA 4720-13 and G. L. was supported by PUCV through Proyecto DI Postdoctorado 2013. C. R. F. was supported by Ministerio de Educación Superior (MES) of Cuba. G. L. wishes to thank his colleagues at the Instituto de Física, Pontificia Universidad de Católica de Valparaíso for their warm hospitality during the completion of this work.

APPENDIX A: STABILITY ANALYSIS OF THE PURE DE SITTER SOLUTION

In this Appendix we introduce local coordinates for analyzing the stability of the pure de Sitter solution given by the fixed point F.

1. Exponential potential

For the stability analysis of the point F, we introduce the local coordinates,

$$\{x, 1 - y, z\} = \{\hat{x}, \hat{y}, \hat{z}\}\epsilon + \mathcal{O}(\epsilon)^2, \tag{A1}$$

where $\epsilon \ll 1$, and $\hat{y} \geq 0$, $\hat{z} \geq 0$.

Then the evolution of the linear perturbations is given by the equations

$$\hat{x}' = -3\hat{x}, \quad \hat{y}' = -3\hat{y} + \frac{3}{2}\hat{z}, \quad \hat{z}' = 3\alpha\hat{z} - \frac{3\alpha\hat{z}^2}{2\hat{y}}. \tag{A2}$$

The system (A2) admits the first integral $\hat{z}\hat{y}^\alpha = c_1$, where c_1 is an integration constant. Thus we can study the reduced system

$$\hat{x}' = -3\hat{x}, \qquad \hat{y}' = -3\hat{y} + \frac{3}{2}c_1\hat{y}^{-\alpha}. \tag{A3}$$

The system (A3) admits the solution passing by $(\hat{x}_0, \hat{y}_0)$ at time $\tau = 0$ given by

$$\begin{aligned} \hat{x}(\tau) &= \hat{x}_0 e^{-3\tau}, \\ \hat{y}(\tau) &= 2^{-\frac{1}{\alpha+1}}(c_1 - e^{-3(\alpha+1)\tau}(c_1 - 2\hat{y}_0^{\alpha+1}))^{\frac{1}{\alpha+1}}, \end{aligned} \tag{A4}$$

where $c_1 = \hat{z}_0\hat{y}_0^\alpha$, $z_0 = z(0)$. Observe that $c_1 \ll 1$ as far as y_0 and z_0 are small enough. We have $(\hat{x}, \hat{y}, \hat{z}) \to (0, 2^{-\frac{1}{\alpha+1}}(\hat{z}_0\hat{y}_0^\alpha)^{\frac{1}{\alpha+1}}, 2^{\frac{\alpha}{\alpha+1}}(\hat{z}_0\hat{y}_0^\alpha)^{\frac{1}{\alpha+1}})$, as $\tau \to \infty$. Thus, for a given $\delta > 0$, and $\alpha > 0$, it is possible to choose an initial state such that $z_0 y_0^\alpha < 2 \times (\frac{\delta}{5})^{\frac{\alpha+1}{2}}$, which give a final state in a δ neighborhood of the origin. This implies the stability, but not the asymptotic stability of F.

2. Arbitrary potential

For the stability analysis of the point F we introduce the local coordinates

$$\{x, 1 - y, z, s\} = \{\hat{x}, \hat{y}, \hat{z}, \hat{s}\}\epsilon + \mathcal{O}(\epsilon)^2, \tag{A5}$$

where $\epsilon \ll 1$, and $\hat{y} \geq 0$, $\hat{z} \geq 0$. Then the evolution of the linear perturbations is given by the equations

$$\begin{aligned} \hat{x}' &= -3\hat{x} + \sqrt{\frac{3}{2}}\hat{s}, \qquad \hat{y}' = -3\hat{y} + \frac{3}{2}\hat{z}, \\ \hat{z}' &= 3\alpha\hat{z} - \frac{3\alpha\hat{z}^2}{2\hat{y}}, \qquad \hat{s}' = -\sqrt{6}\hat{x}f(0). \end{aligned} \tag{A6}$$

The system (A6) admits the first integral $\hat{z}\hat{y}^\alpha = c_1$, where c_1 is an integration constant. Thus we can analysis the reduced system

$$\hat{x}' = -3\hat{x} + \sqrt{\frac{3}{2}}\hat{s}, \quad \hat{y}' = -3\hat{y} + \frac{3}{2}c_1\hat{y}^{-\alpha}, \quad \hat{s}' = -\sqrt{6}\hat{x}f(0). \tag{A7}$$

The system (A7) admits the solution passing by $(\hat{x}_0, \hat{y}_0, \hat{s}_0)$ at time $\tau = 0$ given by

$$\begin{aligned} \hat{x}(\tau) &= \frac{\sqrt{\frac{3}{2}}\hat{s}_0 e^{-3\tau/2}\sinh(\xi\tau)}{\xi} \\ &\quad + \frac{e^{-3\tau/2}\hat{x}_0(2\xi\cosh(\xi\tau) - 3\sinh(\xi\tau))}{2\xi}, \\ \hat{y}(\tau) &= 2^{-\frac{1}{\alpha+1}}(c_1 - e^{-3(\alpha+1)\tau}(c_1 - 2\hat{y}_0^{\alpha+1}))^{\frac{1}{\alpha+1}}, \\ \hat{s}(\tau) &= \frac{\hat{s}_0 e^{-3\tau/2}(3\sinh(\xi\tau) + 2\xi\cosh(\xi\tau))}{2\xi} \\ &\quad + \frac{(4\xi^2 - 9)e^{-3\tau/2}\hat{x}_0\sinh(\xi\tau)}{2\sqrt{6}\xi}, \end{aligned} \tag{A8}$$

where $\beta = \frac{1}{2}\sqrt{9 - 12f(0)}$.

For the choice $\beta^2 < \frac{9}{4}$, i.e., $f(0) > 0$, $(\hat{x}, \hat{y}, \hat{z}, \hat{s}) \to (0, 2^{-\frac{1}{\alpha+1}}(\hat{z}_0\hat{y}_0^\alpha)^{\frac{1}{\alpha+1}}, 2^{\frac{\alpha}{\alpha+1}}(\hat{z}_0\hat{y}_0^\alpha)^{\frac{1}{\alpha+1}}, 0)$, as $\tau \to \infty$. For $\beta = \pm\frac{3}{2}$, i.e., for $f(0) = 0$, $(\hat{x}, \hat{y}, \hat{z}, \hat{s}) \to (\frac{\hat{s}_0}{\sqrt{6}}, 2^{-\frac{1}{\alpha+1}}(\hat{z}_0\hat{y}_0^\alpha)^{\frac{1}{\alpha+1}}, 2^{\frac{\alpha}{\alpha+1}}(\hat{z}_0\hat{y}_0^\alpha)^{\frac{1}{\alpha+1}}, \hat{s}_0)$, as $\tau \to \infty$. Combining the above arguments we obtain that for $f(0) \geq 0$, F is stable, but not asymptotically stable. For $\beta^2 > \frac{9}{4}$, i.e., $f(0) < 0$, the perturbation values $\hat{x}$ and $\hat{s}$ diverges, and $(\hat{y}, \hat{z}) \to (2^{-\frac{1}{\alpha+1}}(\hat{z}_0\hat{y}_0^\alpha)^{\frac{1}{\alpha+1}}, 2^{\frac{\alpha}{\alpha+1}}(\hat{z}_0\hat{y}_0^\alpha)^{\frac{1}{\alpha+1}})$, as $\tau \to +\infty$. Thus, F is a saddle for $f(0) < 0$.

APPENDIX B: CENTER MANIFOLD CALCULATIONS FOR AN SCALAR FIELD WITH EXPONENTIAL POTENTIAL

For analyzing the stability of the curve of critical points G (which exists only for $\lambda = 0$) we introduce the new coordinates

$$\begin{aligned} u_1 &= \frac{y_c(2y(y_c^2 - \alpha - 1) + y_c(-y_c^2 + z + 2\alpha + 1))}{\alpha + 1}, \\ v_1 &= x, \\ v_2 &= -\frac{(y_c^2 - \alpha - 1)(2yy_c - y_c^2 + z - 1)}{\alpha + 1}, \end{aligned} \tag{B1}$$

which are referred to an arbitrary point at G with coordinates $(0, y_c, 1 - y_c^2)$. Applying the procedure, we find that the center manifold is given by the graph

$$\begin{aligned} \Big\{(u_1, v_1, v_2):\ & v_1 = \mathcal{O}(5), \\ & v_2 = \frac{u_1^2(y_c^2 - \alpha - 1)}{4y_c^2(\alpha + 1)} + \frac{u_1^3(y_c^2 - \alpha - 1)}{8y_c^2(\alpha + 1)^2} \\ & \quad + \frac{5u_1^4(y_c^2 - \alpha - 1)}{64y_c^2(\alpha + 1)^3} + \mathcal{O}(5), |u_1| < \delta\Big\}, \end{aligned} \tag{B2}$$

where δ is a small enough constant, and $\mathcal{O}(5)$ denotes terms of five order in the vector norm. The dynamics on the center manifold is governed by the equation

$$u_1' = \mathcal{O}(5).$$

From this follows that G is stable but not asymptotically stable. The center manifold of K is given by the approximated graph

$$\left\{(x, y, z): x = \frac{u^2\lambda}{\sqrt{6}} + \mathcal{O}(5), y = u, \right. \\ \left. z = 1 - \frac{u^4(\alpha-1)\lambda^2}{6(\alpha+1)} - u^2 + \mathcal{O}(5), |u| < \delta\right\}, \tag{B3}$$

where $\mathcal{O}(5)$ denote terms of order 5 with respect the vector norm.

The dynamics on the center manifold of K is dictated by the gradientlike equation

$$u' = -\frac{u^3\lambda^2}{2} + \mathcal{O}(5). \tag{B4}$$

Since the origin is a degenerated minimum of the potential $U(u) = \frac{u^4\lambda^2}{8}$ follows the stability of K.

APPENDIX C: CENTER MANIFOLD CALCULATIONS FOR AN SCALAR FIELD WITH ARBITRARY POTENTIAL

For study the stability of G we resort the Center Manifold Theory. Let us assume that $0 < f(0) \leq \frac{4}{3}$. Then, introducing the new variables

$$\begin{aligned} u_1 &= \frac{y_c(2y(y_c^2 - \alpha - 1) + y_c(-y_c^2 + z + 2\alpha + 1))}{\alpha + 1}, \\ v_1 &= -\frac{(y_c^2 - \alpha - 1)(2yy_c - y_c^2 + z - 1)}{\alpha + 1}, \\ v_2 &= \frac{s\left(\sqrt{6 - 8f(0)y_c^2} - \sqrt{6}\right) + 4f(0)x}{2\sqrt{6 - 8f(0)y_c^2}}, \\ v_3 &= \frac{s\sqrt{6 - 8f(0)y_c^2} - 4f(0)x + \sqrt{6}s}{2\sqrt{6 - 8f(0)y_c^2}}, \end{aligned} \tag{C1}$$

and applying the procedure, we find that the center manifold is given by the graph

$$\{(u_1, v_1, v_2, v_3): v_1 = g(u_1) + \mathcal{O}(5), v_2 = \mathcal{O}(5), \\ v_3 = \mathcal{O}(5), |u_1| < \delta\}, \tag{C2}$$

where $g(u_1) = \frac{u_1^2(5u_1^2 + 8u_1(\alpha+1) + 16(\alpha+1)^2)(y_c^2 - \alpha - 1)}{64y_c^2(\alpha+1)^3}$, δ is a small enough constant, and $\mathcal{O}(5)$ denotes terms of five order in the vector norm.

The dynamics on the center manifold is governed by the equation

$$u_1' = \mathcal{O}(5).$$

Form this follows that G is stable but not asymptotically stable.

For analyzing the case of complex eigenvalues ($f(0) > \frac{4}{3}$), we can introduce the new variables

$$V_2 = \frac{v_2 + v_3}{2}, \qquad V_3 = \frac{v_2 - v_3}{2i},$$

for deriving the real Jordan form of the Jacobian. The procedure is straightforward and the result is the same.

For analyzing the stability of the curve of critical points K we proceed as follows.

Let us assume $s_c \neq 0$. Introducing the new variables

$$\begin{aligned} u_1 &= s - s_c - \sqrt{\frac{3}{2}}xf(s_c), \qquad u_2 = y, \\ v_1 &= \sqrt{\frac{3}{2}}xf(s_c), \qquad v_2 = z, \end{aligned} \tag{C3}$$

and applying the procedure, we find that the center manifold is given by the graph

$$\left\{(u_1, u_2, v_1, v_2): v_1 = \frac{1}{3}s_c u_2^2 + \frac{1}{3}u_1 u_2^2 f(s_c) + \mathcal{O}(4), \right. \\ \left. v_2 = -u_2^2 + \mathcal{O}(4), u_1^2 + u_2^2 < \delta\right\}, \tag{C4}$$

where δ is a small enough constant, and $\mathcal{O}(4)$ denotes terms of fourth order in the vector norm. But since $v_2 \equiv z \geq 0$, it follows that u_2 should be zero. Thus, the center manifold of the origin is

$$\{(u_1, u_2, v_1, v_2): u_2 = 0, v_1 = \mathcal{O}(4), v_2 \\ = \mathcal{O}(4), u_1^2 + u_2^2 < \delta\}. \tag{C5}$$

The dynamics on the center manifold is governed by the equations

$$u_1' = \mathcal{O}(4). \tag{C6}$$

From this fact follows the stability (but not the asymptotic stability) of the center manifold of the origin, thus, follow the stability (but not asymptotic stability) of K.

[1] A. G. Riess *et al.*, Astrophys. J. **116**, 1009 (1998).
[2] S. Perlmutter *et al.*, Astrophys. J. **517**, 565 (1999).
[3] M. Sullivan, Lect. Notes Phys. **800**, 59 (2010).
[4] P. J. E. Peebles and B. Ratra, Rev. Mod. Phys. **75**, 559 (2003).
[5] D. N. Spergel *et al.*, Astrophys. J. Suppl. Ser. **148**, 175 (2003).

[6] M. Tegmark *et al.*, Phys. Rev. D **69**, 103501 (2004).
[7] I. Zlatev, L.-M. Wang, and P. J. Steinhardt, Phys. Rev. Lett. **82**, 896 (1999).
[8] G. Gabadadze, Nucl. Phys. B, Proc. Suppl. **171**, 88 (2007).
[9] E. J. Copeland, M. Sami, and S. Tsujikawa, Int. J. Mod. Phys. D **15**, 1753 (2006).
[10] C. Wetterich, Nucl. Phys. **B302**, 668 (1988); B. Ratra and P. J. E. Peebles, Phys. Rev. D **37**, 3406 (1988); C. Armendariz-Picon, V. Mukhanov, and P. J. Steinhardt, Phys. Rev. Lett. **85**, 4438 (2000); Phys. Rev. D **63**, 103510 (2001); T. Chiba, T. Okabe, and M. Yamaguchi, Phys. Rev. D **62**, 023511 (2000).
[11] R. R. Caldwell and E. V. Linder, Phys. Rev. Lett. **95**, 141301 (2005).
[12] R. J. Scherrer and A. A. Sen, Phys. Rev. D **77**, 083515 (2008).
[13] D. Adak, D. Majumdar, and S. Pal, arXiv:1210.2565; G. Gupta, S. Majumdar, and A. A. Sen, Mon. Not. R. Astron. Soc. **420**, 1309 (2012); S. Dutta and R. J. Scherrer, Phys. Lett. B **704**, 265 (2011); S. del Campo, V. H. Cardenas, and R. Herrera, Phys. Lett. B **694**, 279 (2011); M. Roshan and F. Shojai, Phys. Rev. D **80**, 043508 (2009); S. Sen, A. A. Sen, and M. Sami, Phys. Lett. B **686**, 1 (2010); G. Gupta, E. N. Saridakis, and A. A. Sen, Phys. Rev. D **79**, 123013 (2009); S. Dutta, E. N. Saridakis, and R. J. Scherrer, Phys. Rev. D **79**, 103005 (2009); T. Chiba, Phys. Rev. D **79**, 083517 (2009); **80**, 109902(E) (2009).
[14] M. C. Bento, O. Bertolami, and A. A. Sen, Phys. Rev. D **66**, 043507 (2002).
[15] N. Bilic, G. B. Tupper, and R. D. Viollier, Phys. Lett. B **535**, 17 (2002).
[16] V. Gorini, A. Kamenshchik, and U. Moschella, Phys. Rev. D **67**, 063509 (2003).
[17] M. C. Bento, O. Bertolami, and A. A. Sen, Phys. Rev. D **67**, 063003 (2003).
[18] U. Debnath, A. Banerjee, and S. Chakraborty, Classical Quantum Gravity **21**, 5609 (2004).
[19] Z.-H. Zhu, Astron. Astrophys. **423**, 421 (2004).
[20] X. Zhang, F.-Q. Wu, and J. Zhang, J. Cosmol. Astropart. Phys. 01 (2006) 003.
[21] W. Chakraborty and U. Debnath, Astrophys. Space Sci. **313**, 409 (2008).
[22] A. A. Sen and R. J. Scherrer, Phys. Rev. D **72**, 063511 (2005).
[23] T. Barreiro and A. A. Sen, Phys. Rev. D **70**, 124013 (2004).
[24] A. Ali, S. Dutta, E. N. Saridakis, and A. A. Sen, Gen. Relativ. Gravit. **44**, 657 (2012).
[25] J. C. Fabris, H. E. S. Velten, and W. Zimdahl, Phys. Rev. D **81**, 087303 (2010).
[26] S. del Campo and J. R. Villanueva, Int. J. Mod. Phys. D **18**, 2007 (2009).
[27] J. D. Barrow, Nucl. Phys. **B310**, 743 (1988).
[28] J. D. Barrow, Phys. Lett. B **235**, 40 (1990).
[29] J. Bhadra and U. Debnath, Eur. Phys. J. Plus **127**, 30 (2012).
[30] N. Mazumder, R. Biswas, and S. Chakraborty, Int. J. Theor. Phys. **51**, 2754 (2012).
[31] S. Li, Y. Ma, and Y. Chen, Int. J. Mod. Phys. D **18**, 1785 (2009).
[32] J. He, Y.-B. Wu, and M.-H. Fu, Chin. Phys. Lett. **25**, 347 (2008).
[33] P. Rudra, R. Biswas, and U. Debnath, Astrophys. Space Sci. **339**, 53 (2012).
[34] E. J. Copeland, A. R. Liddle, and D. Wands, Phys. Rev. D **57**, 4686 (1998).
[35] J. J. Halliwell, Phys. Lett. B **185**, 341 (1987).
[36] T. Barreiro, E. J. Copeland, and N. J. Nunes, Phys. Rev. D **61**, 127301 (2000).
[37] A. B. Burd and J. D. Barrow, Nucl. Phys. **B308**, 929 (1988).
[38] M. Sami, P. Chingangbam, and T. Qureshi, Phys. Rev. D **66**, 043530 (2002).
[39] E. Piedipalumbo, P. Scudellaro, G. Esposito, and C. Rubano, Gen. Relativ. Gravit. **44**, 2611 (2012).
[40] C. Rubano and P. Scudellaro, Gen. Relativ. Gravit. **34**, 307 (2002).
[41] I. P. C. Heard and D. Wands, Classical Quantum Gravity **19**, 5435 (2002).
[42] A. A. Coley, J. Ibanez, and R. J. van den Hoogen, J. Math. Phys. (N.Y.) **38**, 5256 (1997).
[43] A. R. Liddle, Phys. Lett. B **220**, 502 (1989).
[44] C. Rubano, P. Scudellaro, E. Piedipalumbo, S. Capozziello, and M. Capone, Phys. Rev. D **69**, 103510 (2004).
[45] Z. K. Guo, Y.-S. Piao, and Y.-Z. Zhang, Phys. Lett. B **568**, 1 (2003).
[46] J. D. Barrow, Phys. Rev. D **49**, 3055 (1994).
[47] J. M. Aguirregabiria, A. Feinstein, and J. Ibanez, Phys. Rev. D **48**, 4662 (1993).
[48] J. M. Aguirregabiria, A. Feinstein, and J. Ibanez, Phys. Rev. D **48**, 4669 (1993).
[49] J. Ibanez, R. J. van den Hoogen, and A. A. Coley, Phys. Rev. D **51**, 928 (1995).
[50] S. A. Pavluchenko, Phys. Rev. D **67**, 103518 (2003).
[51] N. Goheer and P. K. S. Dunsby, Phys. Rev. D **67**, 103513 (2003).
[52] W. Fang, H. Q. Lu, and Z. G. Huang, Int. J. Theor. Phys. **46**, 2366 (2007).
[53] J. M. Aguirregabiria and L. P. Chimento, Classical Quantum Gravity **13**, 3197 (1996).
[54] E. J. Copeland, S. Mizuno, and M. Shaeri, Phys. Rev. D **79**, 103515 (2009).
[55] D. Escobar, C. R. Fadragas, G. Leon, and Y. Leyva, arXiv:1301.2570.
[56] W. Fang, Y. Li, K. Zhang, and H.-Q. Lu, Classical Quantum Gravity **26**, 155005 (2009).
[57] T. Matos, J.-R. Luevano, I. Quiros, L. A. Urena-Lopez, and J. A. Vazquez, Phys. Rev. D **80**, 123521 (2009).
[58] Y. Leyva, D. Gonzalez, T. Gonzalez, T. Matos, and I. Quiros, Phys. Rev. D **80**, 044026 (2009).
[59] L. A. Urena-Lopez, J. Cosmol. Astropart. Phys. 03 (2012) 035.
[60] S. Dutta, E. N. Saridakis, and R. J. Scherrer, Phys. Rev. D **79**, 103005 (2009).
[61] D. Escobar, C. R. Fadragas, G. Leon, and Y. Leyva, Classical Quantum Gravity **29**, 175005 (2012).
[62] D. Escobar, C. R. Fadragas, G. Leon, and Y. Leyva, Classical Quantum Gravity **29**, 175006 (2012).
[63] H. Farajollahi, A. Salehi, F. Tayebi, and A. Ravanpak, J. Cosmol. Astropart. Phys. 05 (2011) 017.

[64] K. Xiao and J.-Y. Zhu, Phys. Rev. D **83**, 083501 (2011).
[65] U. Alam, V. Sahni, T. D. Saini, and A. A. Starobinsky, Mon. Not. R. Astron. Soc. **344**, 1057 (2003); L. Amendola, F. Finelli, C. Burigana, and D. Carturan, J. Cosmol. Astropart. Phys. 07 (2003) 005; X. Zhang, F.-Q. Wu, and J. Zhang, J. Cosmol. Astropart. Phys. 01 (2006) 003; L. Xu and J. Lu, J. Cosmol. Astropart. Phys. 03 (2010) 025; J. Lu, Y. Gui, and L. Xu, Eur. Phys. J. C **63**, 349 (2009); Z. Li, P. Wu, and H. Yu, J. Cosmol. Astropart. Phys. 09 (2009) 017.
[66] N. Liang, L. Xu, Z. H. Zhu, Astron. Astrophys. **527**, A11 (2011); C. G. Park, J. c. Hwang, J. Park, and H. Noh, Phys. Rev. D **81**, 063532 (2010).
[67] L. Xu, J. Lu, Y. Wang, J. Lu, and Y. Wang, Eur. Phys. J. C **72**, 1883 (2012).
[68] A. Del Popolo, F. Pace, S. P. Maydanyuk, J. A. S. Lima, and J. F. Jesus, Phys. Rev. D **87**, 043527 (2013).
[69] S. Lefschetz, *Differential Equations: Geometric Theory* (Dover, New York, 1977).
[70] S. Carloni, P. K. S. Dunsby, S. Capozziello, and A. Troisi, Classical Quantum Gravity **22**, 4839 (2005).
[71] M. Abdelwahab, S. Carloni, and P. K. S. Dunsby, Classical Quantum Gravity **25**, 135002 (2008).
[72] B. Aulbach, *Continuous and Discrete Dynamics near Manifolds of Equilibria*, Lecture Notes in Mathematics Vol. 1058 (Springer, New York, 1984).
[73] V. Sahni and L.-M. Wang, Phys. Rev. D **62**, 103517 (2000).
[74] V. Sahni and A. A. Starobinsky, Int. J. Mod. Phys. D **9**, 373 (2000).
[75] J. E. Lidsey, T. Matos, and L. A. Urena-Lopez, Phys. Rev. D **66**, 023514 (2002).
[76] C. Wetterich, Nucl. Phys. **B302**, 668 (1988).
[77] B. Ratra and P. J. E. Peebles, Phys. Rev. D **37**, 3406 (1988).
[78] T. Matos and L. A. Urena-Lopez, Classical Quantum Gravity **17**, L75 (2000).